Stability Experiment of the High-Speed Active Magnetic Bearing-Flywheel System in the Rotating Frame

Jinpeng Yu [1,2,3], Yan Zhou [1,2,3], Haoyu Zuo [1,2,3], Kai Zhang [4], Pingfan Liu [2,3], Yanbao Li [5], Pengcheng Pu [1,2,3], Lei Zhao [1,2,3], and Zhe Sun[*1,2,3]

[1] Institute of Nuclear and New Energy Technology
[2] Collaborative Innovation Center of Advanced Nuclear Energy Technology
[3] The Key Laboratory of Advanced Reactor Engineering and Safety
[4] Department of Engineering Physics
Tsinghua University, Beijing, 100084, China
yu-jp15@mails.tsinghua.edu.cn, sun_zhe@mail.tsinghua.edu.cn*

[5] Shanghai Aerospace Control Technology Institute
Shanghai, 200000, China

Abstract ─ The active magnetic bearings (AMBs) can greatly improve the stability of the flywheel system and increase the maximum flywheel speed. However, if the active magnetic bearing-flywheel system (AMB-FS) is placed in a rotating frame, the strong gyroscopic effect of high-speed flywheel will greatly affect the system stability. In this study, to realize the high stability of the AMB-FS at ultra-high flywheel speed with low power consumption, the cross feedback PID control was applied in the AMB-FS. The system stability and the performance of AMBs were studied. In the experiment, the gyroscopic effect of the flywheel was effectively suppressed. In the vacuum environment, the flywheel could runs stably at any speed within the range of 0 to 30000 rpm, and the power consumption of AMBs was only 17.82 W and the system had no need of cooling measures. The flywheel speed could exceed 31200 rpm and still possessed the speeding potential. The rotating frame test showed that the maximum frame rotational speed could reach 3.5 deg/s at the rated flywheel speed of 30000 rpm, and the AMB-FS run stably.

Index Terms ─ Active magnetic bearing, cross feedback control, gyroscopic effect, system stability.

I. INTRODUCTION

The active magnetic bearing-flywheel system (AMB-FS) is a nonlinear system with multiple coupling variables. The rotor imbalance, gyroscopic effect and external disturbance will bring about high control requirement for AMBs. Especially in the high-speed AMB-FS, the strong gyroscopic effect of the flywheel will impose a great burden on AMBs and bring about the problem of stability and stability margin [1]. The AMB controller will fail to meet the control requirements and only small external disturbance acting on the high-speed flywheel will lead to the instability of the AMB-FS.

Combining PID controller with other control methods can achieve good control performance. Displacement cross feedback and speed cross feedback can suppress the gyroscopic effect of the flywheel significantly [2]. Zhang [3] implemented the control arithmetic which included cross feedback based on PD controller on the spacecraft attitude control. Reference [4] designed an H∞ controller with gain adjustment, which could suppress the gyroscopic effect significantly. Studies in [5-6] combined variable gain controller with other control methods to stabilize the AMB-FS. All the methods could effectively suppress the gyroscopic effect and improved the system stability. Meanwhile, accounting the uncertainty and robust control will also contribute to improve the control performance and system stability. Reference [7] derived the nominal model of active magnetic suspension of rotor and the uncertainty model, and proposed a robust control with a multi-objective controller to achieve good robust stability when the model of a plant was uncertain. Reference [8] presented the sensitivity and stability margin analyses of the flexible rotor supported by AMBs with the robust optimal vibrations control, and the μ-controller was verified in experimental tests and possessed good performance. References [9-10] proposed an identification method for flexible rotor suspended by magnetic bearings to estimate the unknown parameters and establish the transfer function matrix model of the AMB system, and finally eliminated the influence of bearing stiffness and improved the system stability.

The study in this paper mainly focused on the stability

of the AMB-FS on movable base. The rotating frames accounting the gyroscopic effects is a typical problem, so the AMB-FS in the rotating frame was studied. Furthermore, the PID controller with cross feedback was studied to discover if the controller worked well in the proposed AMB-FS. And with the optimized design of the structure and controller, the performance of AMBs was studied in the experiment. In the second section, the flywheel stability and cross feedback PID controller is analyzed and designed. The third section shows the experiment result of the stability of AMB-FS under cross feedback PID control. The experiment of the high-speed AMB-FS in rotating frame is presented in section four.

II. STABILITY ANALYSIS AND CONTROLLER DESIGN

If the system frame rotates in the different direction from flywheel, the gyroscopic effect of the high-speed flywheel will impose a great burden on AMBs, which will seriously affect the flywheel stability and raise strict control requirements for AMBs. Therefore, for the AMB-FS, the rotating frame can also be equivalent to the external disturbance. The system stability is analyzed based on the horizontal AMB-FS, whose weight is supported by radial AMBs.

A. Stability Analysis

The system mainly includes flywheel, AMB system, drive motor, frame, and other appended structures. The three-dimensional (3D) structure of the AMB-FS is shown in Fig. 1. The system has an inner rotor structure with radial AMBs mounted on the outside of the flywheel, which achieves high inertia ratio of 1.93. The rated flywheel speed is 500 Hz.
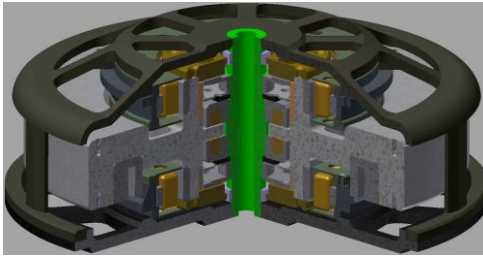
(a) 3D structure of the AMB-FS

(b) The flywheel

Fig. 1. The structure of AMB-FS and flywheel.

Neglecting the influence of the flexible modes of the flywheel, the rigid body model and the force conditions are shown in Fig. 2. The high-speed flywheel is placed horizontally. Since the radial and axial AMBs in the system are decoupled, only the radial AMBs are analyzed.
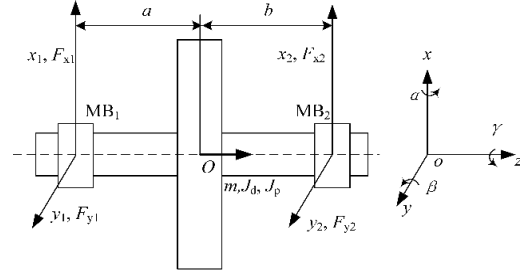

Fig. 2. The flywheel model and the force condition.

$MB_i(i = 1,2)$ are radial AMBs. The flywheel coordinate is $q = [x, \beta, y, -\alpha]^T$ and the AMB coordinate is $q_b = [x_1, x_2, y_1, y_2]^T$, which have the transformation relation $q_b = L_q q$, where,

$$L_q = \begin{bmatrix} 1 & -a & 0 & 0 \\ 1 & b & 0 & 0 \\ 0 & 0 & 1 & -a \\ 0 & 0 & 1 & b \end{bmatrix}. \quad (1)$$

a and b are the distance between radial AMBs and the flywheel centroid. In order to simplify the calculation, it is considered that the displacement sensor and AMBs have the same position. So the motion differential equation of the flywheel is:

$$\begin{cases} m\ddot{x} = F_{x_1} + F_{x_2} + F_{x1}^t + F_{x2}^t \\ m\ddot{y} = F_{y_1} + F_{y_2} + F_{y1}^t + F_{y2}^t \\ J_d\ddot{\alpha} = a(F_{y_1} + F_{y1}^t) - b(F_{y_2} + F_{y2}^t) - J_p\Omega\dot{\beta} \\ J_d\ddot{\beta} = b(F_{x_2} + F_{x1}^t) - a(F_{x_1} + F_{x2}^t) + J_p\Omega\dot{\alpha} \end{cases}, \quad (2)$$

with m the mass of flywheel, x and y the displacements of the flywheel centroid, α and β the rotation angles in the x and y directions, J_d and J_p the diameter and polar moment of inertia and Ω the flywheel speed. $F_{x_1}, F_{x_2}, F_{y_1}$ and F_{y_2} are the electromagnetic forces. $F_{tx_1}, F_{tx_2}, F_{ty_1}$ and F_{ty_2} are the external forces (disturbances). The flywheel is place in the closed frame, so $F_{x1}^t = F_{x2}^t = F_{y1}^t = F_{y2}^t = 0$.

The motion differential equation of the AMB-FS can be rewrite in matrix form:

$$M\ddot{q} + G\dot{q} = L_F F, \quad (3)$$

where $M = \text{diag}(m, J_d, m, J_d)$, $F = [F_{x_1}, F_{x_2}, F_{y_1}, F_{y_2}]^T$, $L_F = L_q^T$ and,

$$G = \begin{bmatrix} 0 & 0 & 0 & 0 \\ 0 & 0 & 0 & 1 \\ 0 & 0 & 0 & 0 \\ 0 & -1 & 0 & 0 \end{bmatrix} J_p\Omega. \quad (4)$$

Let $I = \text{diag}(1,1,1,1)$. The AMB force can be linearized as $F = K_x q_b + K_i I_c$, where $K_x = k_x I$ and

$K_i = k_i I$ are force-displacement and force-current stiffness matrices respectively. Under PID current feedback control, the AMB current is:

$$I_c = -G_s G_i \left(K_p q_b + K_d C \dot{q}_b \right.$$
$$\left. + K_I \int q_b \, dt \right), \tag{5}$$

where $G_s = g_s I$ and $G_i = g_i I$ the coefficients of the displacement sensor and power amplifier, $K_p = k_p I$ and $K_d = k_d I$ the parameter matrices of the PID controller. The matrix C is the cross feedback coefficient. Substitute the AMB force into equation (3) and obtain equation (6):

$$M \ddot{q} + N \dot{q} + V q + W \int q \, dt = 0, \tag{6}$$

where $W = L_F K_i G_s G_i K_I L_q$, $N = G + L_F K_i G_s G_i K_d C L_q$, and $V = L_F K_i G_s G_i K_p L_q - L_F K_s L_q$. The state space equation of the system can be obtained as:

$$\dot{p} = Ap, \tag{7}$$

where $p = (\dot{q}, q, \int q \, dt)^T$ and,

$$A = \begin{bmatrix} -M^{-1}N & -M^{-1}V & -M^{-1}W \\ I & 0 & 0 \\ 0 & I & 0 \end{bmatrix}. \tag{8}$$

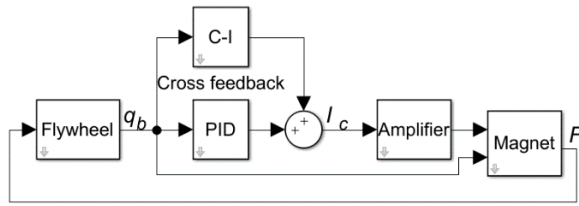Figure 3 shows the PID closed loop system and Table 1 shows the parameters in the simulation.

Fig. 3. The closed loop system with cross feedback.

Under dynamic condition, the flywheel speed has $\Omega \neq 0$. Suppose that the flywheel is under the decentralized PID control ($C = C_d = I$). When the flywheel speed increases from $0\,\text{Hz}$ to $500\,\text{Hz}$, the eigenvalues of matrix A change with the flywheel speed. During the acceleration period, matrix A has three negative real eigenvalues and three pairs of conjugate eigenvalues. The negative real eigenvalues, $a_1^d = -141.2218$, $a_2^d = -96.1456$ and $a_3^d = -1.0178$ remain unchanged. However, the three pairs of conjugate eigenvalues, a_{4i}^d, a_{5i}^d and $a_{6i}^d (i = 1,2)$, are greatly affected by the flywheel speed, as shown in Fig. 4.

Table 1: The parameters in the simulation

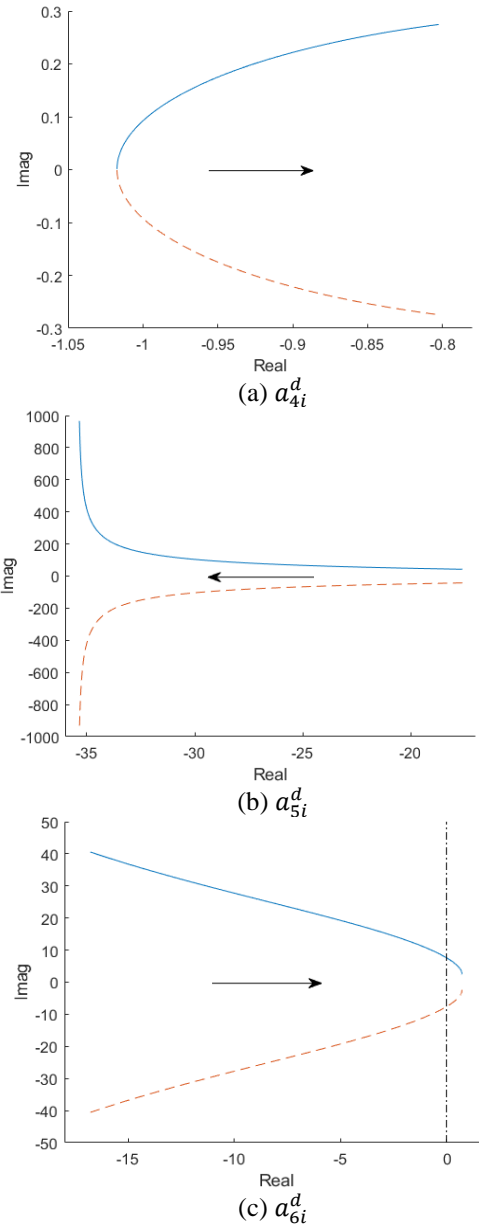| Parameter	Value	Parameter	Value
$a(\text{m})$	0.02	$m(\text{kg})$	5.2
$b(\text{m})$	0.02	$k_x(\text{N/m})$	8982.6
$J_d(\text{kg} \cdot \text{m}^2)$	0.014	$k_i(\text{N/A})$	4.5
$J_p(\text{kg} \cdot \text{m}^2)$	0.027	k_p	9980.7
g_i	1	k_{in}	0.0138
g_s	1	k_d	13.8

(a) a_{4i}^d

(b) a_{5i}^d

(c) a_{6i}^d

Fig. 4. The conjugate eigenvalues change as the flywheel speed up.

As the flywheel speeds up, a_{5i}^d moves away from the imaginary axis, while a_{4i}^d and a_{6i}^d approach the imaginary axis. Therefore, a_{4i}^d and a_{6i}^d become the dominant eigenvalues for the system as the flywheel speeds up. When a_{4i}^d and a_{6i}^d approach the imaginary axis, the absolute value of the real part decrease and the system stability will be decreased significantly. When the flywheel speed is near $450\,\text{Hz}$, the real part of a_{6i}^d turns into positive value and the AMB-FS is instability. Therefore, the original PID controller possesses good robustness under static state but fails to ensure the stability of AMB-FS at high flywheel speed.

B. Controller design

In order to improve the stability of the high-speed AMB-FS, the decentralized PID control was combined with cross feedback control in the actual experiment. The cross feedback suppressed the precession and nutation frequency by taking the displacement signal in the orthogonal direction as the feedback, as shown in Fig. 5.
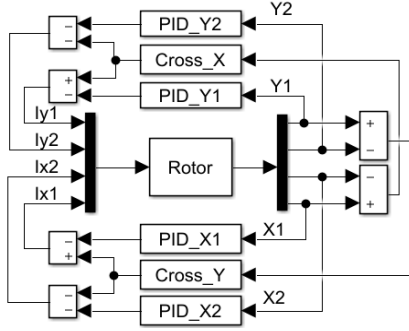

Fig. 5. PID controller with cross feedback.

As for precession, the cross feedback with low-pass characteristics, whose gain in the middle and high frequency band is very low, can effectively damp the precession and has little effect on nutation:

$$G_l = \frac{k_{cl}}{T_{lp}s + 1}. \tag{9}$$

As for nutation, the cross feedback with high-pass characteristics, whose gain in the low frequency band is very low, can effectively damp the nutation and has little effect on procession:

$$G_h = \frac{k_{ch}s}{T_{hp}s + 1}. \tag{10}$$

In order to suppress both the nutation and precession, it is necessary to add the both displacement cross feedback simultaneously, and connect the low-pass and high-pass filters to the corresponding control channel. Therefore, the actual transfer function of the cross feedback is:

$$G(s) = \frac{k_d}{T_{lp}s + 1} + \frac{k_{ch}s}{T_{hp}s + 1}. \tag{11}$$

III. STABILITY EXPERIMENT

Figure 6 shows the AMB-FS experiment platform. The horizontal AMB-FS was placed in the frame, and the frame was placed on a rotatable base. During the running of the AMB-FS, the frame could rotate in the x direction.

A. Static suspension

Figure 7 shows the axis orbit of the flywheel in static suspension. It can be seen that AMBs could suspend the flywheel stably in the static state, and the radial displacement of the flywheel was less than 1 μm.

Fig. 6. Experiment platform.

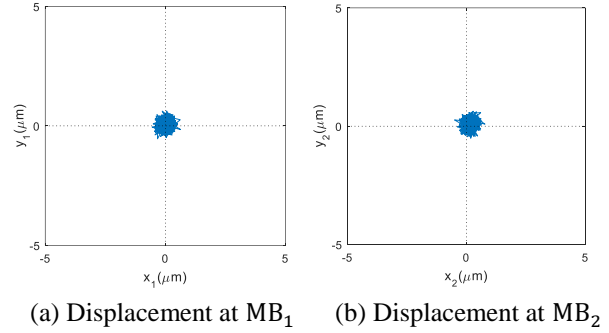(a) Displacement at MB_1 (b) Displacement at MB_2

Fig. 7. Flywheel axis orbit under static suspension.

B. Gyroscopic effect suppression

When the flywheel speed is high, the precession frequency gradually drops to zero, and the nutation frequency increases continually. It is difficult for the decentralized PID controller to effectively suppress the procession and nutation simultaneously. The performance of the cross feedback PID control on the gyroscopic effect was studied in the following experiment.

Figure 8 shows the axis orbit and displacement spectrum of the flywheel without cross feedback control. When the flywheel speed was 40 Hz, the precession was unstable and the decentralized PID controller cannot provide enough damping for the precession mode.

Similarly, without cross feedback control, the nutation was unstable when the flywheel speed was 110 Hz, as is shown in Fig. 9. The nutation frequency is 210 Hz, and the ratio between the nutation frequency and the rotor speed is 1.91, which is basically equal to the inertia ratio of the flywheel [11].
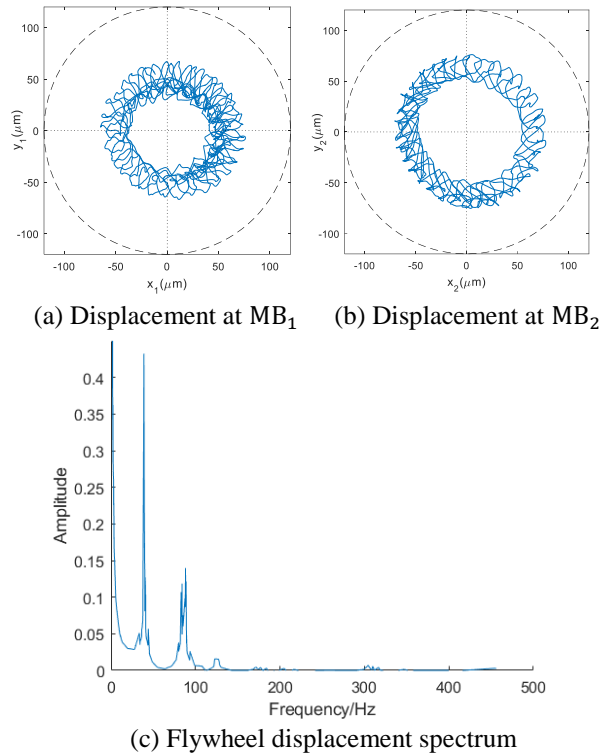
(a) Displacement at MB₁   (b) Displacement at MB₂

(c) Flywheel displacement spectrum

Fig. 8. Precession instability in the experiment.

(a) Displacement at MB₁   (b) Displacement at MB₂
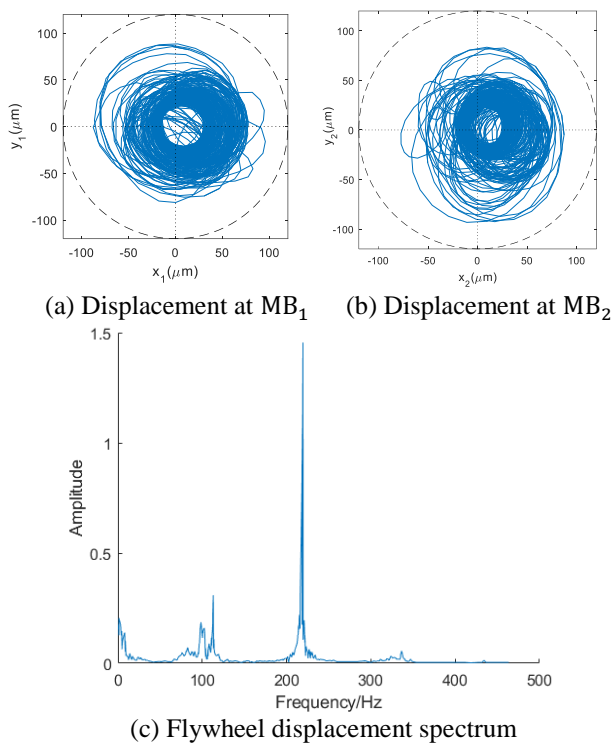

(c) Flywheel displacement spectrum

Fig. 9. Nutation instability in the experiment.

In order to effectively suppress the nutation and precession modes of the flywheel simultaneously, the cross feedback control was introduced. The speed-up experiment of AMB-FS was carried out after selecting the appropriate parameters for the cross feedback PID controller. Figure 10 shows the axis orbit and displacement spectrum of the flywheel. It can be seen that under cross feedback PID control, the procession and nutation modal frequencies were effectively suppressed simultaneously. The AMB controller showed good performance and the AMB-FS was highly stable.

(a) Displacement at MB₁   (b) Displacement at MB₂

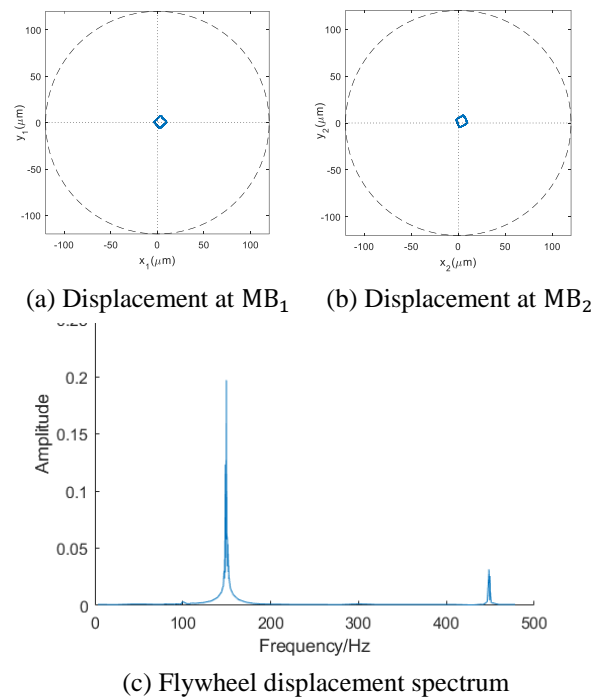(c) Flywheel displacement spectrum

Fig. 10. Stable suspension with cross feedback.

The dashed circle in Figs. 7 and 8 represent the clearance of AMBs. Before the flywheel was totally unstable and had contact with the touchdown bearings, we recorded the data shown in Figs. 7 and 8 and stopped accelerating the flywheel in case of serious damage to the system. If the flywheel runs stably, its axis orbit should be similar with Fig. 6, which means the flywheel has very little displacement in x and y directions. However, in the experiment, as the flywheel speeds up without cross feedback control, its axis orbit changed from Fig. 6 to Figs. 7 and 8, which is the divergent behavior before the flywheel is totally unstable.

In the experiment, the flywheel speed could exceed 31200 rpm and still possessed the speeding potential. When the flywheel rotated at the rated speed of 500 Hz in the vacuum environment, the power consumption of AMBs was only 17.82 W and the system had no need of cooling measures. The radial vibration amplitude of the flywheel was less than 2 μm, and the shaking intensity of the AMB-FS base is less than 0.016 mm/s.

C. Rotating frame experiment

From the theoretical analysis above, it can be seen that the rotating frame leads to strong gyroscopic effect of the flywheel at high speed, which will reduce the AMB controller performance significantly. The flywheel may collide with the touchdown bearings, leading to the instability of the AMB-FS. Therefore, in the rotating frame, the stability of the AMB-FS was analyzed in the experiment.

In the experiment, the flywheel was suspended stably at the rated speed of 500 Hz, and the frame rotated in the x direction at different angular velocity. The axial orbit of both ends of the flywheel and the flywheel displacement spectrum is shown in Fig. 11, where the angular velocity of the frame is 1 deg/s, 1.5 deg/s and 2.5 deg/s, respectively.

(a) 1 deg/s

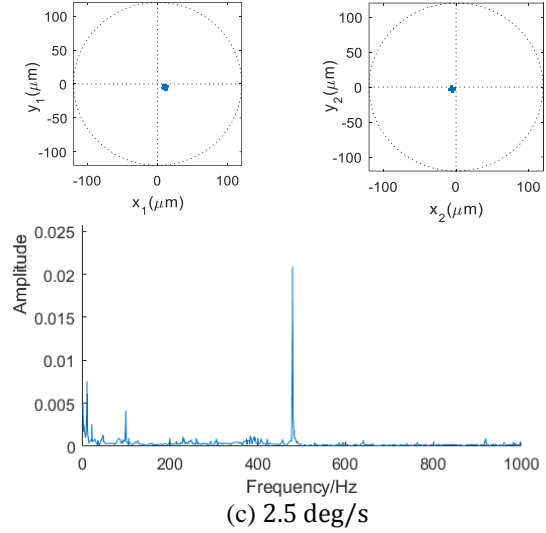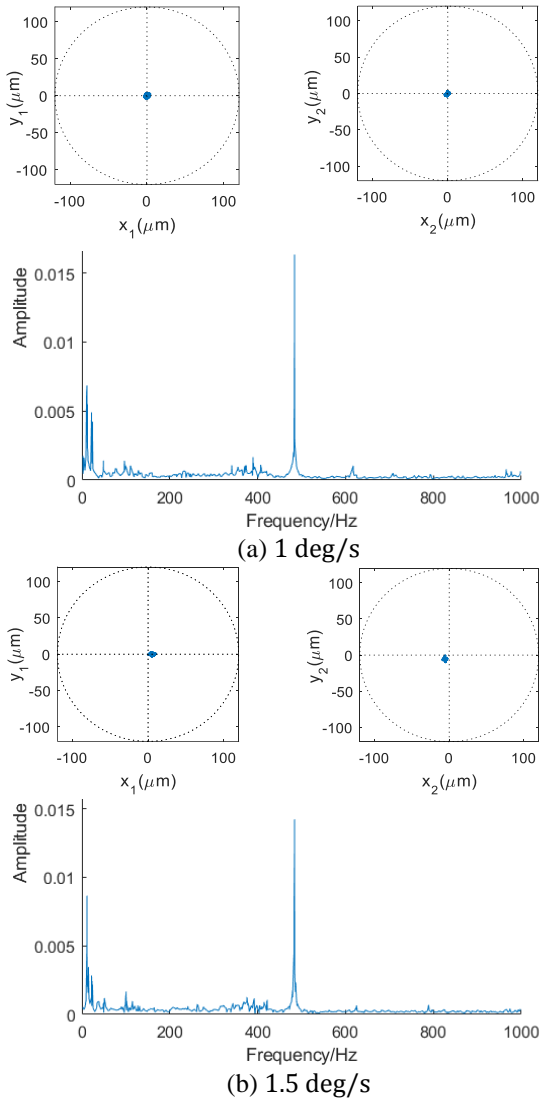(b) 1.5 deg/s

(c) 2.5 deg/s

Fig. 11. Axis orbit and displacement frequency.

From the experimental results, it can be seen that the increase of the frame rotational speed had no effect on the stability of the AMB-FS. There as little change in the flywheel axis orbit and the displacement spectrum. It proves that the cross feedback PID controller possessed good robustness and had high performance in resisting the disturbance of the rotating frame. The dynamic stability of the ultra-high AMB-FS was fully verified under the disturbance of the rotating frame in the experiment.

IV. AMB-FS ANALYSIS IN ROTATING FRAME

Since the power amplifier has maximum current and the ferromagnetic material has saturation magnetization, AMBs have the maximum force. Influenced by the gyroscopic effect and limited by the maximum AMB force, the frame has the maximum rotational speed when the AMB-FS is stable. Therefore, the experiment of the AMB-FS in the rotating frame was studied.

Assume that the rotational angle of the frame is $\theta = \omega_n t + \theta_0$, where θ_0 is the initial angle and ω_n is the frame rotational speed. Under the conditions of small-angle change, the AMB force at time t is:

$$\begin{cases} F_{x_1} = -(k_1 x_1 + d_1 \dot{x}_1) \\ F_{x_1} = -(k_2 x_2 + d_2 \dot{x}_2) \\ F_{y_1} = -[k_3(y_1 - a\theta) + d_3(\dot{y}_1 - a\omega_n)]' \\ F_{y_2} = -[k_4(y_2 + b\theta) + d_4(\dot{y}_2 + b\omega_n)] \end{cases} \quad (12)$$

where k_j $(j = 1, 2, 3, 4)$ and d_j are the stiffness and damping of AMBs. Substitute the equation (12) into the (2) and obtain the ordinary differential equations with

the bearing coordinates $q_b = [x_1, x_2, y_1, y_2]^T$ as the variables, and the solution of equation is:

$$\begin{cases} x_1 = -\dfrac{J_p \Omega \omega_n}{(a+b)k_1} \\ x_2 = \dfrac{J_p \Omega \omega_n}{(a+b)k_2} \\ y_1 = a(\omega_n t + \theta_0) \\ y_2 = -b(\omega_n t + \theta_0) \end{cases} \qquad (13)$$

Therefore, the AMB force can be obtained by substituting equation (13) into equation (12):

$$\begin{cases} F_{x_1} = \dfrac{J_p \Omega \omega_n}{(a+b)} \\ F_{x_1} = -\dfrac{J_p \Omega \omega_n}{(a+b)} \\ F_{y_1} = F_{y_2} = 0 \end{cases} \qquad (14)$$

It can be seen from the result that when the frame rotates in x direction at speed ω_n, there is no force in y direction while the forces in x direction have the same values and opposite directions. The AMB force in x direction is proportional to the product of flywheel speed and frame rotational speed. Therefore, when the flywheel speed is high, only a small frame rotational speed will consume a large amount of AMB force and lead to the force saturation, which will affect the stability of the AMB-FS significantly.

A. Maximum frame speed

AMBs in this study can provide a maximum electromagnetic force of 1200 N. Therefore, with equation (11) and the model in Fig. 5, the relationship between flywheel speed and maximum frame rotational speed can be obtained in Fig. 12, where the solid line is theoretical result and the dotted line is simulation result.

The maximum frame rotational speed was verified in the experiment. The flywheel was placed horizontally, which means its axis was in the horizontal direction and its weight was supported by the radial AMBs. The AMB-FS was placed on a rotatable base.

  A. The flywheel accelerated to a certain speed and run stably.
  B. As the flywheel rotated stably, accelerated the base slowly.
  C. When the base accelerated to the speed at which the flywheel vibrated violently, recorded the speeds of the flywheel and base.
  D. Changed the speed of flywheel and repeated the step A to C.

The dashed line in Fig. 12 shows the experiment result. It can be seen that the results of theory, simulation and experiment agree well. As the flywheel speed increases, the maximum frame rotational speed decreases rapidly.
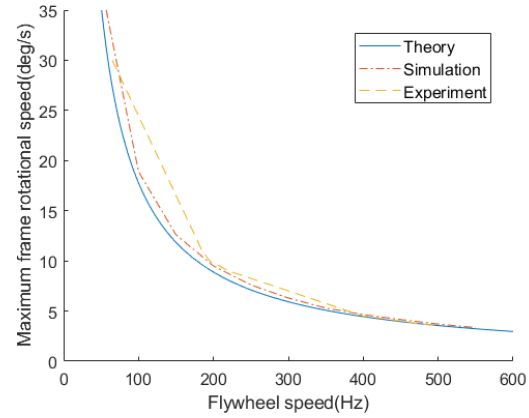

Fig. 12. Relationship between flywheel speed and frame rotational speed.

The experimental results show the high stability of the AMB-FS at high flywheel speed. And the maximum frame rotational speed could reach 3.5 deg/s at the rated flywheel speed of 500 Hz. In the experiment, AMBs needed to provide extra force to offset the flywheel gravity. Therefore, If the flywheel is placed vertically, which means the axis of the flywheel is vertical direction and the weight is supported by axial AMBs, the robustness of AMB controller and the maximum frame rotational speed will be further improved.

B. Features of the AMB Force

In can be seen in the theoretical analysis that the AMB force had different performance in different directions. Therefore, the simulation and the experiment were carried out to observe the features of the AMB force when the frame rotational speed increased. In the simulation, the flywheel rotated at the rated speed of 500 Hz, and the frame rotational speed gradually increased from 0 deg/s to 3.5 deg/s. Figure 13 shows the simulation results of frame rotational speed and the AMB force.

According to theoretical analysis, when the frame rotates in the x direction, AMBs will generate force in x direction to suppress the gyroscopic effect of the flywheel. As shown in Fig. 13 (b), the AMB electromagnetic forces in x direction increased as the frame rotational speed increase, and the force direction of two AMB is opposite. While in the y direction there was only a certain exciting force at the start and stop state of the frame acceleration. The results are consistent with theoretical analysis. Furthermore, in the simulation, the acceleration of the frame was reflected by the flywheel rotating in x direction. Therefore, there was no AMB force in the y direction during the acceleration of the frame.

(a) Frame rotational speed

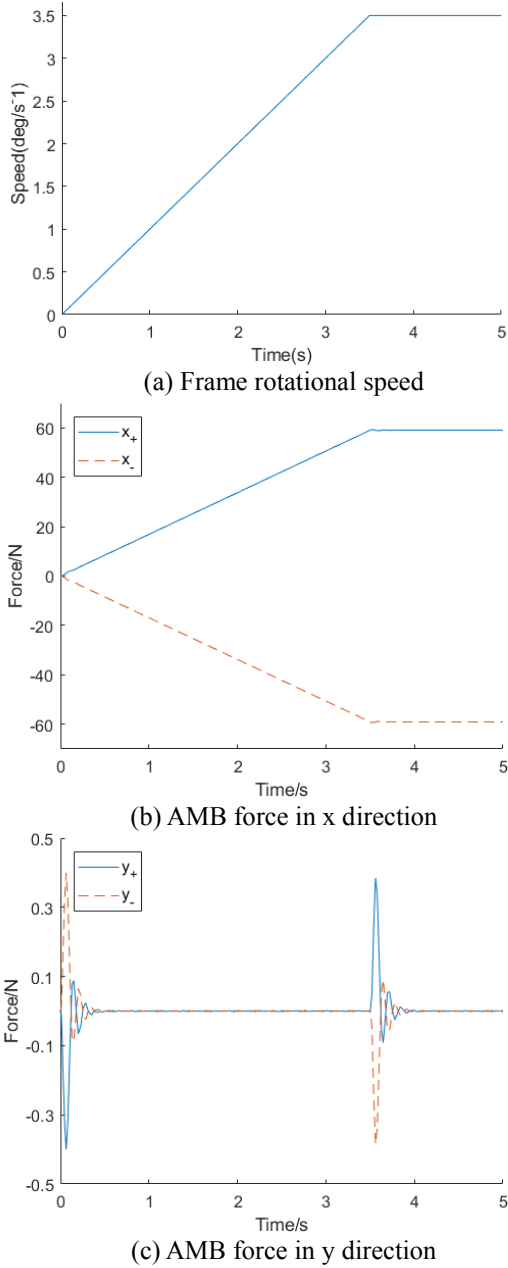(b) AMB force in x direction

(c) AMB force in y direction

Fig. 13. Frame rotational speed and AMB force.

Similarly, in the experiment, the flywheel was suspended stably and rotates at 100 Hz. Recorded the control current of radial AMB when the frame rotated at different rotational speeds. According to the theoretical analysis, when the flywheel rotated in the rotating frame, there is no AMB force in y direction. Therefore, only the control current in x direction was studied in the experiment. By gradually increasing the frame rotational speed until the AMB force was saturate, the features of the AMB force was obtained as Fig. 14 shows.

From the experimental results, it can be seen that the AMB control current changed with the frame rotational

speed. The high-speed flywheel could be suspended stably and the axis orbit was small, so the flywheel displacement could be regarded as a constant. The features of the AMB force can be obtained as Fig. 15 shows. F_{x_1} and F_{x_2} are the AMB force of MB_1 and MB_2, and the $F_{x_i}^+$ points to the positive direction of the x-axis while the $F_{x_i}^-$ points to the negative.

1) When the frame rotational speed is low, the influence of the gyroscopic effect on the AMB-FS is small. The AMB forces $F_{x_1}^+$ and $F_{x_2}^+$ are large, while $F_{x_1}^-$ and $F_{x_2}^-$ are zero. Therefore, the electromagnetic force is mainly used to offset the flywheel gravity.

2) As the frame rotational speed increases, $F_{x_1}^+$ increase rapidly and $F_{x_2}^+$ decreases to zero. The flywheel is in the cantilever state, with the flywheel gravity is use to suppress the gyroscopic effect.

3) When frame rotational speed is high, the external disturbances caused by the gyroscopic effect aggravates. $F_{x_1}^+$ continues to increase while $F_{x_2}^-$ starts to increase. AMBs at both ends of the flywheel provide electromagnetic force to suppress the gyroscopic effect.
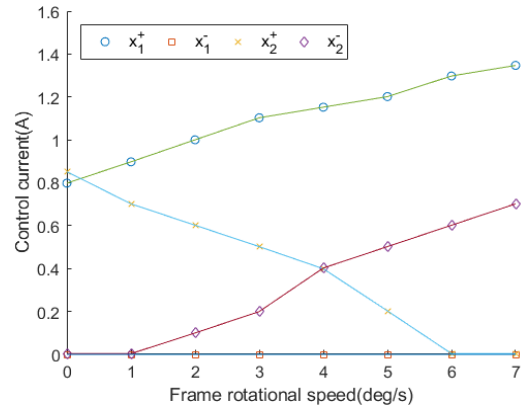

Fig. 14. The AMB control current in x direction.

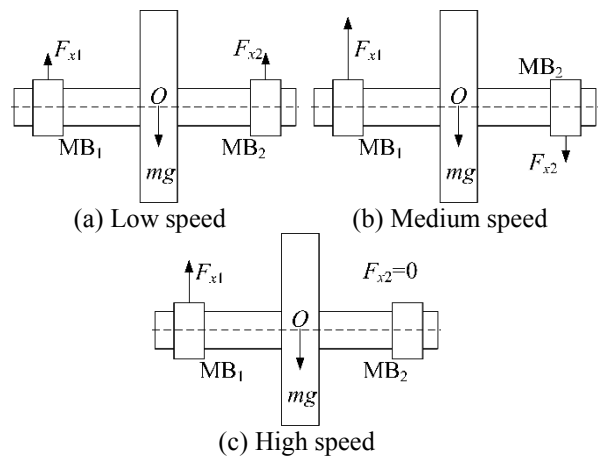(a) Low speed   (b) Medium speed

(c) High speed

Fig. 15. The AMB force under different frame rotational speed.

The resultant force of AMBs is constant, but the resultant moment about the flywheel centroid increases as the frame speeds up to suppress gyroscopic effect. The experimental results agree with the theoretical analysis and show the features of the AMB force when the frame rotational speed increases.

C. Stability at maximum frame speed

As AMBs suppresses the gyroscopic effect caused by the rotating frame, it still need to resist the external disturbance loaded on the flywheel. So the simulation was carried out to observe the influence of external disturbance on the AMB-FS in the rotating frame. When the flywheel rotated at the rated speed of 500 Hz and the frame rotated at the maximum speed of 3.5 deg/s, loaded the external disturbance on the flywheel in the x direction at 6 s. Increased the frame rotational speed to 3.5 deg/s before 4 s, and loaded 58 N external disturbance when the AMB-FS runs stably as shown in Fig. 16 (a), The AMB-FS could return to steady state. However, to suppress the gyroscopic effect, the AMB control current in the x direction was very large and the control current reached saturation during the flywheel returning to the steady state. When the external disturbance came to 60 N, the system was unstable and AMBs cannot meet the control requirement, as shown in Fig. 16 (b).

(a) 58 N in x direction
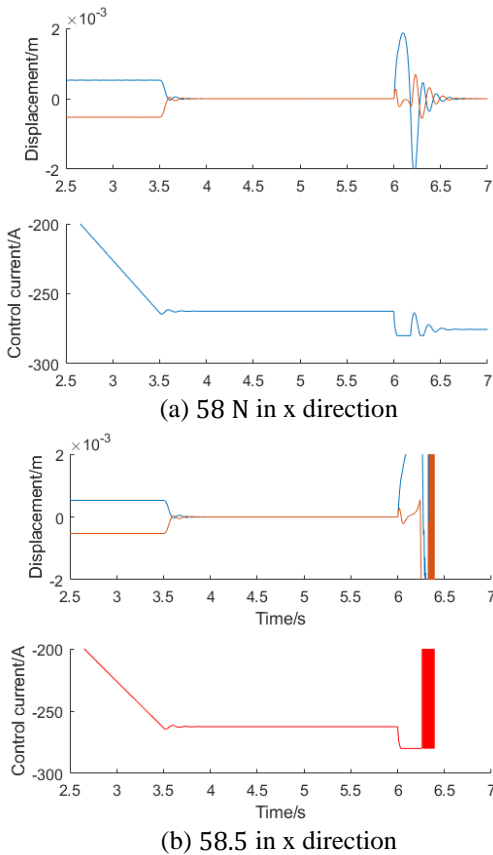

(b) 58.5 in x direction

Fig. 16. Displacement and control current in x direction.

Similarly, repeated the experiment and loaded the external disturbance on the flywheel in the y direction. Increased the frame rotational speed to 3.5 deg/s before 4 s, and loaded 17.5 N external disturbance on the flywheel at 6s. As the Fig. 17 (a) shows, the AMB-FS could return to the steady state. However, the AMB control current in the x direction still reached saturation. When the external disturbance was only 18 N, the system was unstable.

As is known in the theoretical analysis, when the AMB-FS runs in the rotating frame, AMBs in y direction need not to provide electromagnetic force. Therefore, theoretically, the external disturbance loaded in the y direction can be large. However, due to the gyroscopic effect of the flywheel, the external disturbance loaded in the y direction will still seriously affect AMBs in x direction.

(a) 17 N in y direction
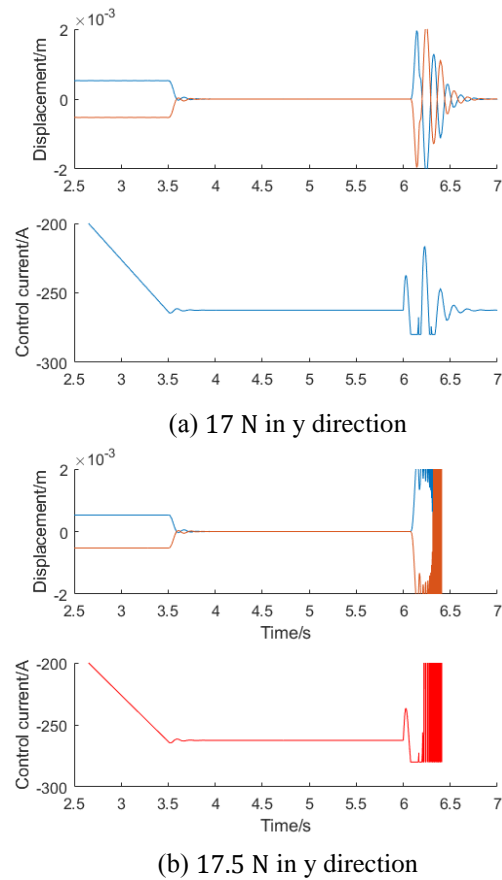

(b) 17.5 N in y direction

Fig. 17. Displacement and control current in x direction.

From the simulation and the analysis, it can be seen that AMBs in the x direction is under seriously requirement regardless of direction of the external disturbance. The external disturbance is against the frame rotational speed. The larger the frame rotational speed, the more the electromagnetic force is consumed to suppress the gyroscopic effect. Therefore, AMBs will

be weak to resist the external disturbance when the frame speed is high. Limited by the experimental conditions, the experiment of external disturbance will be carried out after optimizing the experiment platform.

V. CONCLUSION

In this paper, through stability analysis, AMB controller design, stability experiment and AMB-FS performance experiment, the AMB-FS was designed and studied. The stability of the AMB-FS and the high performance of AMBs were studied in the rotating frame.

➢ Under cross feedback PID control, the gyroscopic effect of the flywheel was effectively suppressed.

➢ The flywheel could be suspended stably at any speed within the range of 0 to 30000 rpm in the vacuum environment, and the AMB-FS showed high stability.

➢ The flywheel speed could exceed 31200 rpm and still possessed the speeding potential.

➢ When the flywheel rotated at the rated speed of 500 Hz in the vacuum environment, the power consumption of AMBs was only 17.82 W and the system had no need of cooling measures.

➢ The radial vibration amplitude of the flywheel was less than 2 μm, and the shaking intensity of the AMB-FS base was less than 0.016 mm/s.

➢ The maximum frame rotational speed at different flywheel speeds was analyzed, and the maximum frame speed could reach 3.5 deg/s at the rated flywheel speed of 500 Hz.

The dynamic and parametric uncertainties of the AMB-FS would be carried out in the further experiment. To reduce the energy loss and improving the stability of the high-speed AMB-FS, the study about the resistance moment of AMBs would be carried out.

REFERENCE

[1] P. C. Pu, J. P. Yu, and L. Zhao, "Analysis of stiffness and damping properties of active magnetic bearing using cross feedback control," *International Conference on Mechanics and Mechanical Engineering*, 2017.

[2] Z. Kai, Z. Lei, and H. Zhao, "Research on control of flywheel suspended by active magnetic bearing system with significant gyroscopic effects," *Chinese Journal of Mechanical Engineering*, pp. 63-66, 2004.

[3] K. Zhang, R. Zhu, and H. Zhao, "Experimental research on a momentum wheel suspended by active magnetic bearings," *Proceedings of the 8th ISMB, Mito*, 2002.

[4] S. Sivrioglu, "Lmi based gain scheduled h_∞ controller design for amb systems under gyroscopic and unbalance disturbance effect," *Proc. Int. Symp. on Magnetic Bearings*, pp. 191-196, 1996.

[5] F. Matsumura, T. Namerikawa, K. Hagiwara, and M. Fujita, "Application of gain scheduled H∞ robustness controllers to a magnetic bearing," in *IEEE Transactions on Control Systems Technology*, vol. 4, no. 5, pp. 484-493, Sep. 1996.

[6] P. Tsiotras and S. Mason, "Self-scheduled H∞ controllers for magnetic bearings," *International Mechanical Engineering Congress and Exposition*, Atlanta, GA, pp. 151-158, Nov. 1996.

[7] Z. Gosiewski and A. Mystkowski, "The robust control of magnetic bearings for rotating machinery," *Solid State Phenomena*, vol. 113, pp. 125-130, 2006.

[8] A. Mystkowski, "Sensitivity and stability analysis of mu-synthesis AMB flexible rotor," *Solid State Phenomena*, vol. 164, pp. 313-318, 2010.

[9] Z. Sun, J. Zhao, Z. Shi, and S. Yu, "Identification of flexible rotor suspended by magnetic bearings," *International Conference on Nuclear Engineering*, pp. V002T03A043 - V002T03A043, 2013.

[10] Z. Sun, Y. He, J. Zhao, et al., "Identification of active magnetic bearing system with a flexible rotor," *Mechanical Systems & Signal Processing*, vol. 49, no. 1-2, pp. 302-316, 2014.

[11] F. Jiancheng, *Technology of Magnetic Suspension Control Moment Gyroscope*. Nationnal Defense Industry Press, 2012.

Jinpeng Yu received his B.Sc. degree in 2015 from Dalian University of Technology. Now he is studying for a Ph.D. at the Institute of Nuclear and New Energy Technology, Tsinghua University. He is mainly engaged in active magnetic bearing and its application in flywheel system.

Zhe Sun is currently an Aassociate Professor and Ph.D. Supervisor of Tsinghua University. His research interests are control and monitoring of active magnetic levitation system, rotor dynamics, statistical learning theory and its engineering application, etc. He has published more than 20 SCI/EI index papers and 10 national patents. He presides over and participates in a series of National Science and Technology Major Project of China, National Natural Science Foundation of China and National High-tech Research and Development Program of China.